The Potential of Electrospun Poly(methyl methacrylate) / Polycaprolactone Core-Sheath Fibers for Drug Delivery Applications

Maria Cecília Rodrigues Simões (ORCID: 0000- 0002- 0780- 2773),[a] Simon M. Cragg (ORCID: 0000-0003-1082-7653),[b] Eugen Barbu (ORCID: 0000-0002-2053-4136),[c] Frederico B. De Sousa (ORCID: 0000-0002-7930-6867)[a*]

[a]Laboratório de Sistemas Poliméricos e Supramoleculares (LSPS) - Instituto de Física e Química, Universidade Federal de Itajubá (UNIFEI), Itajubá, 37500-903, MG, Brazil.

[b]Institute of Marine Sciences, School of Biological Sciences, University of Portsmouth, Ferry Road, Portsmouth PO4 9LY, UK.

[c]School of Pharmacy and Biomedical Sciences, University of Portsmouth, St. Michael's Building, White Swan Road, Portsmouth PO1 2DT, UK.

Corresponding author:
Prof. Dr. Frederico B. De Sousa
Laboratório de Sistemas Poliméricos e Supramoleculares (LSPS) - Instituto de Física e Química, Universidade Federal de Itajubá (UNIFEI), Itajubá, 37500-903, MG, Brazil.
55 35 3629175
fredbsousa@gmail.com, fredbsousa@unifei.edu.br

Abstract

Drug-loaded core-sheath fibers were successfully prepared from a combination of poly(methyl methacrylate) (PMMA) and polycaprolactone (PCL) using a coaxial electrospinning system and Nimesulide as an anti-inflammatory drug model. An electric field potential of 7-8 kV was found optimal for the formation of the fibers, which were characterized using scanning and transmission electron microscopy techniques combined with attenuated total reflectance infrared spectroscopy and contact angle measurements. Results confirmed the core-sheath morphology and indicated that these fibers are larger in diameter than normal ones (prepared as controls from either PCL or PMMA, under similar conditions). The prepared core-sheath fibers were also investigated by differential scanning calorimetry (DSC) and thermogravimetric analysis (TGA), and results indicated that Nimesulide is completely solubilized in the polymer matrix and that its presence improved the thermal stability of the core-sheath fibers compared to that of normal PMMA fibers. Moreover, PMMA-PCL core-sheath fibers showed an improvement in terms of mechanical properties (such as elongation at break) in comparison with pure PMMA fibers. Drug release studies demonstrated that the delivery of Nimesulide can be modulated by appropriately selecting the loading area, with faster release observed when the drug was located in the sheath. Results suggest altogether the significant potential of PMMA-PCL core-sheath fibers for applications involving delivery of hydrophobic anti-inflammatory drugs such as Nimesulide.

Key words: Polycaprolactone, Poly(methylmethacrylate), Core-Sheath Fibers, Nimesulide, Electrospinning, Drug Release.

1. Introduction

Electrospinning is a versatile technique capable of processing a wide variety of materials such as ceramics, metals, glass or organic polymers to form fibers with diameters in the nano or micrometre range [1–3], as a result of electrostatic forces caused by the attraction of opposite charges between the solution droplets and the collector [4, 5]. In addition to being non-toxic, biodegradable and biocompatible [6], polymeric fibers used in biomedical applications require other important characteristics such as high surface area, porosity, malleability or mechanical resistance, which confer them the ability to perform appropriately in various roles as drug carriers, for drug solubilization or controlled release [7–11]. Drug-loaded fiber systems have the potential to adjust the drug dissolution range and to modulate the drug dosage, thus eliminating problems with inaccurate dosing while increasing efficacy and reducing toxicity and side effects [12, 13].

Like normal monoaxial fibers, core-sheath (or coaxial) fibers can be generated by electrospinning two solutions simultaneously through a coaxial needle, to form fibers with one type of material inside (the core) and the other one on the outer side (the sheath), as presented in Figure 1. Core-sheath fibers present advantages in comparison to normal ones in terms of their mechanical and biological properties [20–23], as well as in terms of their potential to modulate drug release [24–27]. These fiber systems offer the potential to deliver drugs in a way that avoids side effects found with drugs delivered in solution.

Nimesulide is a hydrophobic anti-inflammatory drug that is a selective COX-2 isoform inhibitor, and it has been approved for use in the symptomatic treatment of severe pain states [14][15]. However, due to the toxicity manifested in its hepatic metabolism, Nimesulide has been strongly regulated and even prohibited in some countries, and novel alternatives for the administration of this drug (such as transdermal systems or semi solid formulations) have been the focus of recent attention [16–19]. Thus, a method of delivery that avoids passage through the hepatic circulation is needed.

Figure 1. a) Schematic representation of the core-sheath fibers electrospinning system.

Poly(methylmethacrylate) (PMMA) is a hydrophobic and amorphous polymer used in a range of biomedical, optical or sensor applications [28]; as a result of its good biocompatibility, PMMA is of particular interest for the delivery of anti-inflammatory and antibiotics drugs in systems such as scaffolds, bone cements, or implants [29].

However, PMMA fibers produced by electrospinning typically have low mechanical strength and require reinforcement [30], and to address this limitation we have considered in this study using polycaprolactone (PCL). PCL is a synthetic but biodegradable and biocompatible polymer that is hydrophobic and semi-crystalline; PCL is approved for use in biomedical applications for several types of devices, and it has been found that it imparts good mechanical properties when used in combination with other polymers [31–34]. Both PMMA and PCL have been suggested in the literature as suitable materials for drug delivery systems [35–37], and it has been found that blends of these polymers can improve the mechanical properties of fibers investigated for the release of dyes employed as model drugs [34].

In this paper we report on the preparation by coaxial electrospinning of novel core sheath-fibers, alternatively loaded with Nimesulide in each of the two layers, and on the evaluation of their potential to deliver such hydrophobic actives. Nimesulide was selected as a model drug as this non-steroidal anti-inflammatory active requires innovative alternatives for its administration due to its significant hepatotoxicity. The coaxial fibers were prepared from a combination of PMMA (core) and PCL (sheath) with the aim to improve their mechanical properties while building in the ability to modulate the drug release. Results of our investigations of drug-polymer interactions are also reported.

2. Experimental Section

2.1 Materials

Polymethylmethacrylate (average Mn = 350,000) and Polycaprolactone (average Mn = 35,000) were purchased from Sigma Aldrich. Nimesulide was locally purchased (Araújo Manipulações Belo Horizonte - MG). Other chemicals, including dimethylformamide (DMF), tethahydrofuran (THF), and dicloromethane (DCM) were obtained from Sigma Aldrich and used without further purification.

2.2 Fabrication of Core-Sheath Fibers by Electrospinning

Normal fibers of pure PMMA and pure PCL were prepared first in order to use them as control materials for comparison with the core sheath fibers. PMMA fibers were prepared using a solution (12 %w) in DMF:THF (7:3 vol), and PCL fibers were prepared using a solution (32 %w) in DCM:DMF (9:1 vol). Concentrations and solvent rations were chosen based on preliminary experiments. Electrospun core sheath fibers were then prepared by combining the above solutions, which were independently but concomitantly

electrosprayed using a coaxial needle. All fibers were prepared using a Spraybase (Avectas) instrument equipped with a programmable syringe pump (World Precision Instruments, Florida, US) and a stainless steel coaxial nozzle (Rame-hart Instrument Co, NJ, US) with an internal needle diameter of 2.11 mm (outer) and 1.07 mm (inner needle). Table 1 presents the parameters used in order to obtain all fiber mats. Where Nimesulide was used, the drug was dissolved separately in the above solutions at a concentration of 6 mg/mL, and two types of fibers were produced: PMMA (core) and PCL (sheath), with core-loaded Nimesulide; and, PMMA (core) and PCL (sheath), with sheath-loaded Nimesulide.

Table 1: Parameters employed in the fabrication of both normal and core-sheath fibers, in the presence or absence of Nimesulide.

2.3 Scanning and Transmission Electron Microscopy studies

Surface morphology of the core sheath fibers were investigated using a JEOL-6060LV scanning electron microscope (JEOL Ltd, Japan) operated at 15 kV. Dried samples were gold coated for 2 min with a Q150R ES sputter (Quorum Technologies Ltd, East Sussex, UK). Samples were also analyzed by transmission electron microscopy using a JEOL-2000FX instrument (JEOL Ltd, Japan) at an operating voltage of 80 kV; samples were deposited on Formvar coated copper grids (200 Mesh). The fibers diameter was determined using at least 60 measurements from three different micrographs, using Image J analysis software.

2.4 Contact angle goniometry

The hydrophobicity of the fibers prepared was investigated on the upper surface of the electrospun fiber mats using a contact angle measuring system G10 (Krüss GmbH, Germany) by means of sessile drop method measurements, at room temperature, using ultrapure water (10 x 10 μL drops). The analysis was performed in triplicate.

2.5 Fourier Transform Infrared Spectroscopy with Attenuated Total Reflectance (FTIR-ATR)

FTIR-ATR spectra were recorded using a Perkin Elmer Spectrum 100 instrument equipped with a diamond crystal ATR module (wavelength range 650 to 4000 cm^{-1}; 4 cm^{-1} resolution; 36 scans).

2.6 Thermal Analysis

Fibers were investigated by differential scanning calorimetry using a DSC-214 Polyma instrument (Netzsch, Germany) equipped with a CC203 liquid nitrogen cooling accessory. Samples (10 mg) were analyzed over a broad temperature range (- 90 to 250 °C) at a heating rate of 10 °C/min, in nitrogen (2 cycles). Fiber samples (about 15 mg) were also investigated by thermogravimetric analysis (TGA), which was performed on a TG-209 F1 instrument (Netzsch, Germany), from 20 to 800 °C under nitrogen flow (50 mL/min), and then in dry air (50 mL/min) from 800 to 1000 °C.

2.7 Water Vapor Permeability

Water vapor permeability (WVP) was measured with a Payne's cup (10 mL) using a method reported in the literature [38, 39]. Distilled water was used and the polymeric fiber samples (cut from the mat obtained by electrospinning as circles with a test area of 0.95 cm^2) were placed in the lid of the cup. The ability of the water vapor to permeate through the fiber mats was correlated with the loss of water inside the cup over time. The system was placed in a desiccator (with silica gel) that generated a humidity gradient across the fiber mat samples mounted in the cup lid. The experiments were performed in triplicate, and the water vapor flow (J) was calculated as following, equation 1:

$$J = \Delta m/\Delta t \times A \quad (1)$$

where $\Delta m/\Delta t$ is the angular coefficient of the mass variation *versus* time (graph obtained from the results of the gravimetric measurements of cups), and A is the sample surface area (cm^2) exposed during the test.

The water vapor permeability (P) was calculated using the equation (2) below:

$$P = J \text{ x } L/\Delta PVx(T) \quad (2)$$

where J was obtained from Eq. (1), L is the membrane thickness, and ΔPV x (T) is the vapor pressure difference (water vapor pressure generate inside of the dessicator) at a given temperature (25 ºC).

2.8 Mechanical Properties

The burst strength of the fiber mats was evaluated using a TA-XT2 texture analyzer instrument (Stable Micro Systems, UK) equipped with a Stable Micro Systems film support rig accessory and a 5 mm stainless steel ball probe (D = 5 mm). The velocity of the probe was 1 $mm.s^{-1}$, with a pre-test speed of 2 $mm.s^{-1}$, and 49 mN as trigger force. The results were expressed as puncture strength (PS) and elongation at break (EB; %), which were calculated according to equations 3 and 4 [38]:

$$Ps = \frac{F}{A} \quad (3)$$

where Ps ($N.mm^{-2}$) is puncture strength, F (N) is the force leading to the rupture of the film and A (mm^2) is the sectional area of the fiber mats used in the experiment. The area was calculated as A = 2*rh*, where *r* (mm) is the radius of the clamping accessory hole and *h* is the fiber mat's thickness;

$$EB = \frac{\sqrt{r^2+d^2}-r}{r} \times 100 \quad (4)$$

where *r* (mm) is the radius of exposed fibers and *d* (mm) is the displacement caused by the applied force. The experiments were performed in triplicate.

2.9 *In vitro* drug release studies

The release of Nimesulide loaded into the core-sheath fibers was evaluated *in vitro* under static diffusion conditions using Franz cells [40–42]. The Nimesulide content in each type of fiber was determined from the electrospinning process parameters using equations 7 and 8. The amount of Nimesulide was found to be 2.552 ±1.60 % for fibers where the drug was loaded in the core and 1.176 ±0.06 % for those where the drug was loaded in the sheath. Samples of both fiber mats were cut with an approximate diffusional area of 1 cm^2, accurately weighed, and then placed in separate Franz cells. For each cell, both compartments were filled with a saline phosphate buffer pH 7.4 (1 mL in the donor compartment and 3.6 - 3.8 mL in the receiving compartment), with a 5×2 mm magnetic stirrer bar added to the receiving compartment. To increase the solubility of the drug in the receiving compartment, 0.1 %w of Soluplus® was added to the saline phosphate buffer solution. Synthetic cellulose acetate membranes (molecular weight cutoff 12–14 kDa) were used to support the fiber mat samples; they were cut into circular pieces (2.4 cm of

diameter) and mounted to adequately cover the receiving chamber. The Franz cells were submerged in a temperature controlled (37 ºC) shaker incubator. For each sample, a set volume (0.4 mL) of liquid from the receptor compartment was sampled at predetermined time intervals, and was replaced by an equal volume of preheated saline phosphate buffer also containing Soluplus®. Samples were analyzed using High Performance Liquid Chromatography (HPLC), performed with an Agilent instrument equipped with a UV detector (Agilent Technologies 1100 series/1200 detector) and a C8 column (4.6 mm x 25 cm) with water/acetonitrile (1:1 v/v) as mobile phase to determine the concentration of each sample collected (Cn). The analysis was performed in triplicate and the cumulative release profile was represented as % Nimesulide released over time (calculated using equation 6):

$$M_t=(C_n \text{ x } V + \sum(C_{n-1}\times 0.4)) \quad (5)$$

$$\%\ \text{drug released} = \frac{M_t}{M_\infty}\ x\ 100 \quad (6)$$

where Mt (µg) is the cumulative mass of drug released up to time point *t* (h), when the n^{th} sample was collected (calculated using equation 5); Cn (µg/mL) is the concentration of the n^{th} sample (as determined by HPLC) and V (mL) is the total volume of the receptor solution in the Franz Cell (V = 3.6 - 3.8 mL). $\sum(C_{n-1}\times 0.4)$ represents the total mass of drug that has been previously removed (with the *n-1* samples that were collected earlier). M_∞ is the total mass of Nimesulide loaded in the sample that was subjected to the test, and has been determined from the concentration (C; g/mL) and flow rate (F; mL/h) of each solution employed in the process of electrospinning, using equations 7 and 8.

$$M_{\infty(\text{Nim core})} = \frac{(F_{PMMA}\times C_{Nimesulide})}{[(F_{PMMA}\times C_{PMMA})+(F_{PCL}\times C_{PCL})+(F_{PMMA}\times C_{Nimesulide})}\times sample\ mass \quad (7)$$

$$M_{\infty(\text{Nim sheath})} = \frac{(F_{PCL}\times C_{Nimesulide})}{[(F_{PMMA}\times C_{PMMA})+(F_{PCL}\times C_{PCL})+(F_{PCL}\times C_{Nimesulide})}\times sample\ mass \quad (8)$$

2.10 Statistical analysis

The results were analyzed using One-way ANOVA followed by Tukey's Multiple Comparison Test, using GraphPad Prism 5.0 software. The subscript letters used in tables indicate the subdivision in groups as a result of Tukey's post-test; differences were considered statistically significant where $p < 0.05$.

3. Results and discussion

3.1 Preparation of core-sheath fibers and morphology investigations

Core-sheath fibers based on a combination of PMMA and PCL were successfully fabricated by electrospinning, with good reproducibility, using a coaxial system, as described in the experimental section. The optimization of the factors that typically influence the electrospinning process [8][43] was carried out in preliminary experiments, and the main parameters are summarized in Table 1. As an example, Figure 2 presents the formation of the Taylor's cone during the electrospinning process of PMMA/PCL core-sheath fibers.

Figure 2. Optical image of the Taylor's cone during the fabrication of the PMMA/PCL core-sheath fibers.

The morphology investigations indicated that all fibers present a well-defined cylindrical shape (Figure 3), without typical drops or beads previously reported in the literature [34]. The diameters of the fibers, as measured from the SEM images, are presented in Table 2. These results are in agreement with similar data reported in the literature that indicate that core-sheath fibers, as a result of the electrospinning setup, are normally larger in diameter than the normal ones [24]; this was confirmed by statistical analysis ($p < 0.05$). Results of TEM studies (Figure 4) endorse the core-sheath morphology of the fibers prepared.

Table 2. The average diameter of the fibers.

Figure 3. SEM images of: a) normal PCL fibers; b) normal PMMA fibers; c) core-sheath fibers of PMMA (core) and PCL (sheath), with core-loaded Nimesulide; d) core-sheath fibers of PMMA (core) and PCL (sheath), with sheath-loaded Nimesulide.

Figure 4. TEM images of the core-sheath fibers with PMMA (core) and PCL (sheath), with core-loaded Nimesulide: a) 800x magnification; b) 3000x magnification (scale bars 20 µm).

3.2 Fourier Transform Infrared Spectroscopy with Attenuated Total Reflectance (FTIR-ATR)

Stretching vibrations associated with the C=O groups present in PMMA and PCL polymers were observed around 1720 cm^{-1}, and those associated with the C–O bonds were observed in the regions 1190-1140 cm^{-1} for PMMA and 1239-1160 cm^{-1} for PCL (Figure 5). C-H stretching and bending vibrations appeared at 3000-2869 cm^{-1} and 1472-1430 cm^{-1}, respectively, in agreement with previous data reported in the literature [44] [45]. Absorption bands characteristic to pure Nimesulide are due to N-H stretching vibrations (3280 cm^{-1}), however these were not clearly observed for the Nimesulide-loaded fibers, likely due to the low concentration of drug present. Consequently, no significant difference was observed between the FTIR spectra of core-sheath fibers having Nimesulide loaded in the core and those having Nimesulide loaded in the sheath. It was however noticeable that the FTIR spectra of the core-sheath fibers were more similar to that of normal PCL, in particular in the C-H stretching region, evidencing the core-sheath structure with PCL as the outer component (considering the maximum penetration depth of up to 2 microns for the ATR technique [46]).

Figure 5. FTIR-ATR spectra of: a) pure Nimesulide; b) normal PMMA fibers; c) normal PCL fibers; d) core-sheath fibers (PMMA core / PCL sheath); e) core-sheath fibers (PMMA core / PCL sheath) with sheath-loaded Nimesulide; f) core-sheath fibers (PMMA core / PCL sheath) with core-loaded Nimesulide.

3.3 Thermal Analysis

The drug-polymer interactions in the prepared core-sheath fibers were investigated by dynamic scanning calorimetry (DSC) [47]. The glass transition temperature (Tg) of PMMA observed in the normal electrospun fibers (110 ºC) is in accordance with literature data [47][28][48], however the observed Tg value for the PMMA/PCL core-sheath fibers (without Nimesulide) was 132 ºC, suggesting a significant constraint in the movements of the PMMA chains. The core-sheath fibers with Nimesulide present in the sheath showed a Tg value of 131 ºC, while the same type of

fibers with Nimesulide located in the core had a Tg value of 105 ºC; the lower value observed for the latter suggests a significant increase in this case in the PMMA polymer chain mobility, similar to observations reported in the literature for polymer matrix based composites [47]. It can be suggested that the presence of a strong polar group (sulphonamide) in the molecule of Nimesulide could interfere with the dominant hydrophobic interactions between PMMA or PCL macromolecules and result in a higher mobility of the polymer chains. Moreover, the fact that no endothermic drug melting peak (near 150 ºC, as characteristic to pure Nimesulide) could be observed in the DSC thermograms of the Nimesulide-loaded core-sheath fibers suggests that the drug is not present in the loaded fibers in its crystalline form [15].

The melting point (Tm) of PCL did not present significant differences for different types of fibers; the Tm value for pure PCL fibers was observed at 60 ºC, and for core-sheath fibers (without drug) at 61 ºC. A similar value (60 ºC) was detected for the core-sheath fibers with Nimesulide alternatively located in each layer.

Figure 6. DSC thermograms for: a) pure Nimesulide; b) normal PCL fibers; c) core-sheath fibers (without drug); d) core-sheath fibers with core-loaded Nimesulide; e) core-sheath fibers (without drug); d) core-sheath fibers with sheath-loaded Nimesulide; and, f) normal PMMA fibers. Left side: expansion for the Tm region characteristic to PCL. Right side: expansion for the Tg region characteristic to PMMA.

Results of thermogravimetric analysis evidenced a two-step thermal degradation of high molecular weight PMMA. The first one, between 200-290 ºC, is likely a result of the homolytic scission of the polymer chain; the second one, between 300-400 ºC, is described in the literature as corresponding to the cleavage of the monomers resulting in the formation of new radicals, quickly degraded *via* random scissions [28][48][49]. For normal, pure PCL fibers, the decomposition was found to occur in a single stage, at 410 ºC, in accordance with literature reports that explain it as a consequence of polyester chain rupture via *cis*-elimination reaction and unzipping depolymerization from the ends of the polymer chain [50].

The first derivative thermograms (dTG, presented in Figure 7) indicate that the peak corresponding to the first degradation step of PMMA appears at a higher temperature in the core-sheath fibers (300 °C) compared to the normal PMMA fibers (287 °C). A similar behavior was observed for the core-sheath fibers loaded with Nimesulide either

in the sheath (320 °C) or in the core (325 °C), demonstrating the presence of drug-polymer interactions that appear to improve the thermal stability of the system.

Figure 7. First derivative thermograms of: a) pure Nimesulide; b) normal PMMA fibers; c) normal PCL fibers; d) core-sheath fibers (no drug); e) core-sheath fibers with sheath-loaded Nimesulide; f) core-sheath fibers with core-loaded Nimesulide.

3.4 Mechanical properties

The results of the determination of puncture strength (PS) and elongation at break (EB) are presented in Table 2. The poor mechanical properties of normal PMMA fibers obtained by electrospinning were evident during the fabrication of these fibers, when breaking could sometimes be observed; the reinforcing effect of PCL, known for its superior mechanical properties, was clearly noticeable. The different thickness of the fiber mats was accounted for using Equation 4, which allowed the calculation of PS and EB values (Table 3). It can be seen that elongation at break was significantly higher for core-sheath fibers when compared to normal PMMA fibers (while still lower than that obtained for pure PCL fibers, though this was to be expected [51][34]).

Table 3. PS and EB values for normal and core-sheath fibers.

3.5 Contact Angle Goniometry

Measurements of the wetting ability of a surface can provide important information on its hydrophilicity [35][52], which is relevant for drug release as this process is ultimately controlled by the interactions between the polymer and the surrounding aqueous medium. Results of contact angle measurements using deionized water droplets revealed lower values for the core-sheath fibers containing Nimesulide compared to pure polymer fibers (Table 4); this indicates that the hydrophilicity of the materials was significantly increased by the addition of the drug, which appears to interact strongly with both polymers as evidenced also by the results of thermal analysis.

Table 4. Results of contact angle measurements for normal and core-sheath fibers.

3.6 Water Vapor Permeability

Water Vapor Permeability (WVP) is indicative of the barrier capacity of the fiber mats, and can be defined as the rate of transmission of water vapor through a flat surface by the unit of thickness, at specified temperature and humidity conditions [53]. The vapor permeation process is driven by the vapor pressure difference across the fiber mat, which acts as a membrane, and the barrier capacity is the result of a combination of several factors such as mat structure and porosity, hydrophilicity, and polymer compatibility [38][54]. The results of thickness and water vapor permeability measurements are presented in Table 5. The core-sheath fibers presented higher WVP values in comparison with normal fibers made of pure polymers. In line with the results obtained from the contact angle measurements, it appears that the presence of Nimesulide makes the fibers more hydrophilic, with a lower contact angle and higher vapor permeability.

Table 5. Results of water vapor permeability (WVP) measurements.

3.7 Drug release studies

Drug release investigations were carried out in Franz cells, in saline phosphate buffer pH 7.4, under static diffusion conditions. The release of Nimesulide was monitored by HPLC and the cumulative drug release data is represented in Figure 8. The content of Nimesulide loaded in the core-sheath fibers was 25.52 mg per g of fiber (when core-loaded) and 11.76 mg per g fiber (when sheath-loaded), as determined using equation 7. Perhaps unsurprisingly, results indicate that the drug release was faster (and more complete) from the fibers where the drug was loaded in the sheath compared to those where the drug was loaded in the core, and where the diffusion path was longer. After 20 h, almost half of the Nimesulide loaded in the sheath was released, in contrast to only about 20 % of the drug loaded in the core. Alongside DSC and TG data, the low levels of drug released suggest the presence of interactions between Nimesulide and the polymer matrices that contribute to the retention of the active.

The release rates were also different, depending on the localization of the drug. In addition to diffusion path length, the nature of the polymer can also have an impact. In agreement with the literature, where it has been suggested that the incorporation and release of a drug from polymer matrices can be influenced by the glass transition temperature (Tg) of the polymer [54][55], a stronger burst effect was observed for the investigated fibers when Nimesulide was loaded in PCL (a polymer with low Tg, - 60 ºC) than in PMMA (higher Tg, 118 ºC). The explanation offered for this effect is associated

with the effect of the rubbery state that can provide a lesser penetration of the low molecular weight drug into the nanopores present in the fibers; diffusion kinetics following a Fickian model have been observed in the first case, while a time dependent non-Fickian behavior was reported in the literature for the latter type of polymers, possibly because of the necessary rearrangement of the polymer chains so they can accommodate the diffusing drug molecules [54][55]. The results demonstrate clearly the ability of these PMMA/PCL coaxial fibers to control the different release rates and released drug levels depending on the localization of the active.

Figure 8. Cumulative *in vitro* drug release profiles from: a) PMMA (core) / PCL and Nimesulide (sheath) fibers; b) PMMA and Nimesulide (core)/PCL (sheath) fibers.

To assess the mechanism of Nimesulide release from the two types of drug-loaded coaxial fibers investigated, the experimental data was fitted to a number of kinetic models such as Hixon and Crowell, Higuchi, Peppas, Baker, first order, or Weibull (Table 6). According to the calculated correlation coefficients r^2 (Table 5), the Nimesulide release data was found to be best described by the Weibull statistical model, typically useful for describing drug release from matrix-type systems. According to this model, a general function - represented in Equation (9) - can be applied successfully to describe the experimental release profiles, with the value of the exponent *b* indicative of the drug release mechanism [55][56].

$$F = 1 - \exp(at^b) \quad (9)$$

where, F = the amount of the drug released; b = shape parameter, a = time parameter. Values of b below 0.75 indicate Fickian diffusion, values between 0.75 and 1.0 indicate non-Fickian diffusion, while values above 1.0 indicate a complex drug release mechanism.

The overall results suggest a Fickian diffusion mechanism for the release of Nimesulide from both types of drug-loaded core-sheath fibers, in agreement with literature reports that indicate that drug release from polymers with a very slow degradation rate (such as PCL) is typically controlled by diffusion [57][58].

Table 6: Mathematical models and fitting parameters for the release profile of Nimesulide from the loaded core-sheath fibers.

4 Conclusions

Core-sheath fibers based on PMMA and PCL and differently loaded with the anti-inflammatory drug Nimesulide were prepared successfully using a coaxial electrospinning technique. Combining PMMA with PCL in coaxial fibers overcomes some of the limitations of the former in terms of mechanical properties by improving characteristics such as elongation at break, and also increases the thermal stability of these fibers compared to that of the pure polymers. The water vapor permeability of the prepared core-sheath fiber mats was found to be higher compared to that of mats fabricated from normal, pure polymer fibers, with the inclusion of Nimesulide as a potential contributing factor. The release of Nimesulide was found to be controlled mainly by Fickian diffusion and to be strongly influenced by the location of the active in the drug-loaded, core-sheath fibers; the active was released faster and at a higher level (almost 50 % over 20 h) when loaded in the sheath compared to when it was located in the core (cumulative release 20 % over 20 h), with a reduced burst effect observed for the latter.

The results suggest altogether that core-sheath fibers fabricated by coaxial electrospinning from hydrophobic polymers such as PMMA and PCL have improved properties compared to normal fibers obtained from pure polymers (particularly PMMA) and can be used to conveniently modulate the release of hydrophobic anti-inflammatory actives such as Nimesulide in prospective drug delivery applications.

5 Acknowledgments

The authors gratefully acknowledge the contribution of Ana Leão Mouquet, Andréia Bagliotti Meneguin, Aikaterini Lalatsa and Marta Roldo to certain experimental aspects and useful discussions. This work was supported by the PDSE programme (CAPES n. 019/2017), FAPEMIG (grant numbers APQ-00134-14 and APQ-00403-17), and CNPq (grant numbers: 312367/2014-7 and 306726/2017-3). This work was financed in part by the Coordenação de Aperfeiçoamento de Pessoal de Nível Superior – BRASIL (CAPES)-Finance Code nº 001. The authors gratefully acknowledge the Federal Institute of South of Minas Gerais - IFSuldeminas for their support.

6 References

1. Greiner A, Wendorff JH (2007) Electrospinning: A fascinating method for the preparation of ultrathin fibers. Angew Chem Int Edit 46:5670–5703
2. Xue J, Xie J, Liu W, Xia Y (2017) Electrospun Nanofibers: New Concepts, Materials, and Applications. Acc Chem Res 50:1976–1987
3. Hu X, Liu S, Zhou G, et al (2014) Electrospinning of polymeric nanofibers for drug delivery applications. J Control Release 185:12–21
4. Sill TJ, Von Recum HA (2008) Electrospinning: Applications in drug delivery and tissue engineering. Biomaterials 29:1989–2006
5. Baji A, Mai YW, Wong SC, et al (2010) Electrospinning of polymer nanofibers: Effects on oriented morphology, structures and tensile properties. Compos Sci Technol 70:703–718
6. Ibrahim I, Sadiku E, Jamiru T, et al (2017) Applications of Polymers in the Biomedical Field. Curr Trends Biomed Eng Biosci 4:9–11
7. Liang D, Hsiao BS, Chu B (2007) Functional electrospun nanofibrous scaffolds for biomedical applications. Adv Drug Deliv Rev 59:1392–1412
8. Pelipenko J, Kocbek P, Kristl J (2015) Critical attributes of nanofibers: Preparation, drug loading, and tissue regeneration. Int J Pharm 484:57–74
9. Chou SF, Carson D, Woodrow KA (2015) Current strategies for sustaining drug release from electrospun nanofibers. J Control Release 220:584–591
10. Munj HR, Tyler Nelson M, Karandikar PS, et al (2014) Biocompatible electrospun polymer blends for biomedical applications. J Biomed Mater Res - Part B Appl Biomater 102:1517–1527
11. Göke K, Lorenz T, Repanas A, et al (2018) Novel strategies for the formulation and processing of poorly water- soluble drugs. Eur J Pharm Biopharm 126:40–56
12. Kumbar SG, Nair LS, Bhattacharyya S, Laurencin CT (2006) Polymeric Nanofibers as Novel Carriers for the Delivery of Therapeutic Molecules. J Nanosci Nanotechnol 6:2591–2607
13. Sebe I, Szabó P, Kállai-Szabó B, Zelkó R (2015) Incorporating small molecules or biologics into nanofibers for optimized drug release: A review. Int J Pharm 494:516–530
14. Rainsford KD (2005) The discovery, development and novel actions of nimesulide. In: Nimesulide - Actions and Uses. Birkhäuser Basel, pp 1–61
15. Huerta C, Aberturas M del R, Molpeceres J (2015) Nimesulide-loaded

nanoparticles for the potential coadjuvant treatment of prostate cancer. Int J Pharm 493:152–160

16. Bessone F (2010) Non-steroidal anti-inflammatory drugs: What is the actual risk of liver damage? World J Gastroenterol 16:5651–5661
17. Marziyeh S, Moghddam M, Ahad A, et al (2017) Optimization of nanostructured lipid carriers for topical delivery of nimesulide using Box – Behnken design approach. Artif Cell Nanomed B 45:617–624
18. Donati M, Conforti A, Lenti MC, et al (2016) Risk of acute and serious liver injury associated to nimesulide and other NSAIDs: data from drug-induced liver injury case–control study in Italy. Br J Clin Pharmacol 238–248
19. Bakhrushina EO, Anurova MN, Smirnov V V., Demina NB (2017) Development of Analytical Methods for Peroral Prolonged-Release Nimesulide Gel. Pharm Chem J 51:130–135
20. Sperling LE, Reis KP, Pranke P, Wendorff JH (2016) Advantages and challenges offered by biofunctional core-shell fiber systems for tissue engineering and drug delivery. Drug Discov Today 21:1243–1256
21. Khalf A, Madihally S V. (2017) Modeling the permeability of multiaxial electrospun poly(??-caprolactone)-gelatin hybrid fibers for controlled doxycycline release. Mater. Sci. Eng. C-Mater. Biol. Appl. 76:161–170
22. Lu Y, Huang J, Yu G, et al (2016) Coaxial electrospun fibers: applications in drug delivery and tissue engineering. Wiley Interdiscip Rev Nanomedicine Nanobiotechnology 8:654–677
23. Qian W, Yu D, Li Y, et al (2013) Triple-Component Drug-Loaded Nanocomposites Prepared Using a Modified Coaxial Electrospinning. J Nanomater 2013:1–7
24. Oliveira MF, Suarez D, Rocha JCB, et al (2015) Electrospun nanofibers of polyCD/PMAA polymers and their potential application as drug delivery system. Mater. Sci. Eng. C-Mater. Biol. Appl. 54:252–261
25. Bonadies I, Maglione L, Ambrogi V, et al (2017) Electrospun core/shell nanofibers as designed devices for efficient Artemisinin delivery. Eur Polym J 89:211–220
26. Castillo-Ortega MM, Nájera-Luna A, Rodríguez-Félix DE, et al (2011) Preparation, characterization and release of amoxicillin from cellulose acetate and poly(vinyl pyrrolidone) coaxial electrospun fibrous membranes. Mater. Sci. Eng. C-Mater. Biol. Appl. 31:1772–1778

27. Najafi-Taher R, Derakhshan MA, Faridi-Majidi R, Amani A (2015) Preparation of an ascorbic acid/PVA–chitosan electrospun mat: a core/shell transdermal delivery system. RSC Adv 5:50462–50469
28. Ali U, Karim KJA, Buang NA (2015) A Review of the Properties and Applications of Poly (Methyl Methacrylate) (PMMA). Polym Rev 55:678–705
29. Bettencourt A (2012) Poly (methyl methacrylate) particulate carriers in drug delivery. J Microencapsul 29:353–367
30. Dong H, Strawhecker KE, Snyder JF, et al (2012) Cellulose nanocrystals as a reinforcing material for electrospun poly(methyl methacrylate) fibers: Formation, properties and nanomechanical characterization. Carbohyd Polym 87:2488–2495
31. Woodruff MA, Hutmacher DW (2010) The return of a forgotten polymer - Polycaprolactone in the 21st century. Prog Polym Sci 35:1217–1256
32. Suwantong O (2016) Biomedical applications of electrospun polycaprolactone fiber mats. Polym Advan Technol 27:1264–1273 . doi: 10.1002/pat.3876
33. Ali Akbari Ghavimi S, Ebrahimzadeh MH, Solati-Hashjin M, Abu Osman NA (2014) Polycaprolactone/starch composite: Fabrication, structure, properties, and applications. J Biomed Mater Res - Part A 103:2482–2498
34. Munj HR, Tomasko DL (2017) Polycaprolactone-polymethyl methacrylate electrospun blends for biomedical applications. Polym Sci Ser A+ 59:695–707
35. Son S-R, Linh N-TB, Yang H-M, Lee B-T (2013) In vitro and in vivo evaluation of electrospun PCL/PMMA fibrous scaffolds for bone regeneration. Sci Technol Adv Mater 14:1–10
36. Kim Y-H, Lee B-T (2011) Novel approach to the fabrication of an artificial small bone using a combination of sponge replica and electrospinning methods. Sci Technol Adv Mater 12:1–7
37. Yoon J, Yang HS, Lee BS, Yu WR (2018) Recent Progress in Coaxial Electrospinning: New Parameters, Various Structures, and Wide Applications. Adv Mater 1704765:1–23
38. Ribeiro SD, Guimes RF, Meneguin AB, et al (2016) Cellulose triacetate films obtained from sugarcane bagasse: Evaluation as coating and mucoadhesive material for drug delivery systems. Carbohydr Polym 152:764–774
39. Bagliotti Meneguin A, Stringhetti Ferreira Cury B, Evangelista RC (2014) Films from resistant starch-pectin dispersions intended for colonic drug delivery. Carbohydr Polym 99:140–149

40. Lalatsa A, Emeriewen K, Protopsalti V, et al (2016) Developing transcutaneous nanoenabled anaesthetics for eyelid surgery. Br J Ophthalmol 100:871–876
41. Zupančič Š, Potrč T, Baumgartner S, et al (2016) Formulation and evaluation of chitosan/polyethylene oxide nanofibers loaded with metronidazole for local infections. Eur J Pharm Sci 95:152–160
42. Wang Q, Wang YZ, Zhao ZF, Fang B (2012) Synthesis of SIS-based hot-melt pressure sensitive adhesives for transdermal delivery of hydrophilic drugs. Int J Adhes Adhes 34:62–67
43. Rasekh M, Young C, Roldo M, et al (2015) Hollow-layered nanoparticles for therapeutic delivery of peptide prepared using electrospraying. J Mater Sci-Mater M 26:1–12
44. Erbas E, Kiziltas A, Bollin SC, Gardner DJ (2015) Preparation and characterization of transparent PMMA – cellulose-based nanocomposites. Carbohyd Polym 127:381–389
45. Abdelrazek EM, Hezma AM, El-khodary A, Elzayat AM (2016) Spectroscopic studies and thermal properties of PCL/PMMA biopolymer blend. Egypt J Basic Appl Sci 3:10–15
46. Khodkar F, Golshan Ebrahimi N (2017) Preparation and properties of antibacterial, biocompatible core–shell fibers produced by coaxial electrospinning. J Appl Polym Sci 134:1–9
47. Liu H, Liu D, Fei Y, Wu Q (2010) Fabrication and properties of transparent polymethylmethacrylate/cellulose nanocrystals composites. Bioresour Technol 101:5685–5692
48. Carrizales C, Pelfrey S, Rincon R, et al (2008) Thermal and mechanical properties of electrospun PMMA, PVC, Nylon 6, and Nylon 6,6. Polym Advan Technol 19:124–130
49. Ferriol M, Gentilhomme A, Cochez M (2003) Thermal degradation of poly (methyl methacrylate)(PMMA): modelling of DTG and TG curves. Polym Degrad Stabil 79:271–281
50. Sivalingam G, Karthik R, Madras G (2003) Kinetics of thermal degradation of poly(ε-caprolactone). J Anal Appl Pyrolysis 70:631–647
51. Suwantong O (2016) Biomedical applications of electrospun polycaprolactone fiber mats. Polym Advan Technol 27:1264–1273
52. Kissa E (1996) Wetting and Wicking. Text Res J 66:660–668

53. Standard Test Methods for Water Vapor Transmission of Materials 1, American Society for Testing and Materials, ASTM 96.
54. Tan B, Thomas NL (2016) A review of the water barrier properties of polymer/clay and polymer/graphene nanocomposites. J Membrane Sci 514:595–612
55. Zupančič Š, Sinha-Ray S, Sinha-Ray S, et al (2016) Long-Term Sustained Ciprofloxacin Release from PMMA and Hydrophilic Polymer Blended Nanofibers. Mol Pharm 13:295–305
56. Langenbucher F (1972) Letters to the Editor: Linearization of dissolution rate curves by the Weibull distribution. J Pharm Pharmacol 24:979–981
57. Repanas A, Glasmacher B (2015) Dipyridamole embedded in Polycaprolactone fibers prepared by coaxial electrospinning as a novel drug delivery system. J Drug Deliv Sci Tec 29:132–142
58. Sultanova Z, Kaleli G, Kabay G, Mutlu M (2016) Controlled release of a hydrophilic drug from coaxially electrospun polycaprolactone nanofibers. Int J Pharm 505:133–138

Table 1: Parameters employed for the fabrication of normal and core-sheath fibers, with and without Nimesulide.

Fibers	**Flow rate of PMMA or PMMA/Nimesulide solution (mL/h)**	**Flow rate of PCL or PCL/Nimesulide solution (mL/h)**	**Collector distance (cm)**	**DC Voltage (kV)**
Normal PMMA	6.0	-	16	6.0
Normal PCL	-	2.0	15	8.5
PMMA/PCL without Nimesulide	3.5	1.5	15	7.0
PMMA (core) and PCL (sheath), with core-loaded Nimesulide	3.5	1.2	15	7.0
PMMA (core) and PCL (sheath), with sheath-loaded Nimesulide	2.5	1.5	15	7.5

Table 2. Results for the diameter of the fibers.

Fibers	**Diameter (㎜)**
Normal PMMA	1.75 ± 0.13 $_{a}$
Normal PCL	1.49 ± 0.24 $_{b}$
PMMA (core) and PCL (sheath), with core-loaded Nimesulide	4.48 ± 0.45 $_{c}$
PMMA (core) and PCL (sheath), with sheath-loaded Nimesulide	3.83 ± 0.34 $_{d}$

Table 3. PS and EB values obtained for the coaxial fibers in comparison to normal fibers.

Fibers	**Thickness (mm)**	**Puncture strength (PS) (MPa)**	**Elongation at break (EB) (%)**
Normal PMMA	0.255 ± 0.04 ^{a}	0.099 ± 0.03 ^{a}	0.125 ± 0.03 ^{a}
Normal PCL	0.223 ± 0.05 ^{a}	0.662 ± 0.21 ^{b}	11.039 ± 2.22 ^{b}
PMMA (core) and PCL (sheath), with core-loaded Nimesulide	1.167 ± 0.02 ^{b}	0.279 ± 0.03 ^{a}	2.943 ± 0.32 $^{a, c}$
PMMA (core) and PCL (sheath), with sheath-loaded Nimesulide	1.073 ± 0.03 ^{c}	0.242 ± 0.02 ^{a}	3.450 ± 0.92 ^{c}

Table 4. Results of contact angle measurements for normal and core-sheath fibers.

Fibers	**Contact angle**
Normal PMMA	146 ± 1.4 [a, c]
Normal PCL	152 ± 0.8 [a]
PMMA (core) and PCL (sheath), with core-loaded Nimesulide	125 ± 0.8 [b, d]
PMMA (core) and PCL (sheath), with sheath-loaded Nimesulide	122 ± 2.6 [c, d]

Table 5. Results of water vapor permeability (WVP) measurements.

Fibers	**WVP** (10^{-4} **g.mm.h^{-1}.m^{-2}.KPa^{-1})**	**Thickness (mm)**
Normal PMMA	$0.39 \pm 0.04_{a}$	$0.2538 \pm 0.02_{a}$
Normal PCL	$0.68 \pm 0.06_{a}$	$0.5021 \pm 0.04_{b}$
PMMA (core) and PCL (sheath), with core-loaded Nimesulide	$1.39 \pm 0.13_{b}$	$0.3633 \pm 0.04_{a, c}$
PMMA (core) and PCL (sheath), with sheath-loaded Nimesulide	$1.25 \pm 0.04_{b}$	$0.3366 \pm 0.01_{c}$

Table 6: Mathematical models and curve fitting parameters for the Nimesulide release profiles (core-sheath fibers).

Mathematical models	**PMMA (core) and PCL (shell), with shell-loaded Nimesulide**	**PMMA (core) and PCL (shell), with core-loaded Nimesulide**
Hixon and Crowell	$r^2 = 0.259$ $k = 3x10^{-4}$	$r^2 = 0.7123$ $k = 6.84x10^{-5}$
Higuchi	$r^2 = 0.8223$ $k = 1.7115$	$r^2 = 0.9396$ $k = 0.5528$
Peppas	$r^2 = 0.8839$ $k = 3.9403$ $n = 0.3656$	$r^2 = 0.9372$ $k = 0.4096$ $n = 0.5477$
Baker	$r^2 = 0.8782$ $k = 6.45x10^{-5}$	$r^2 = 0.9378$ $k = 5.43x10^{-6}$
First order	$r^2 = 0.4028$ $k = 0.011$	$r^2 = 0.7282$ $k = 0.0002$
Weibull	$r^2 = 0.9955$ $k = 9.17x10^{-2}$ $b = 0.01347$	$r^2 = 0.9989$ $k = 41.0687$ $b = 0.0113$

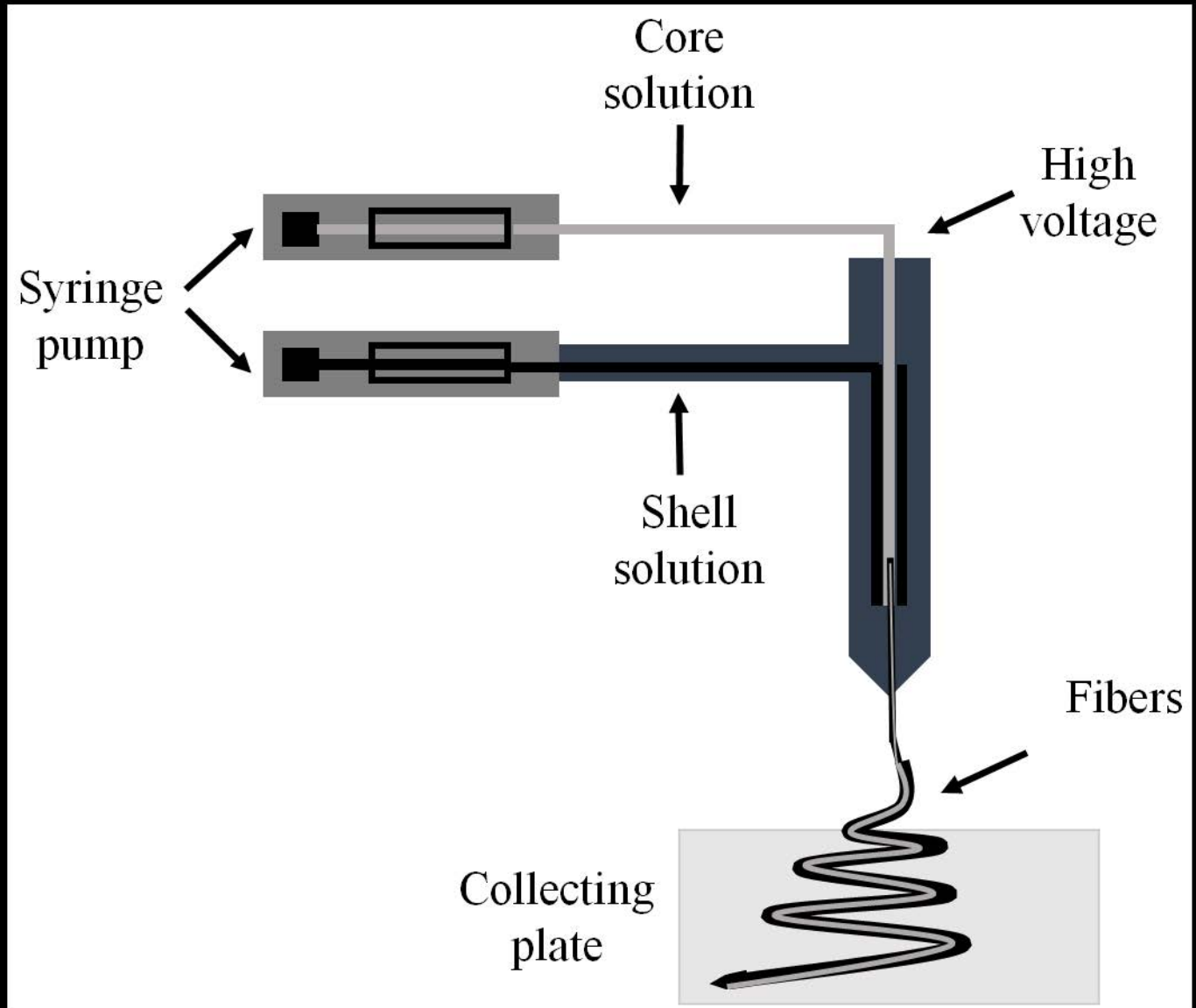
Core
solution
High
voltage
Syringe
pump
Shell
solution
Fibers
Collecting
plate

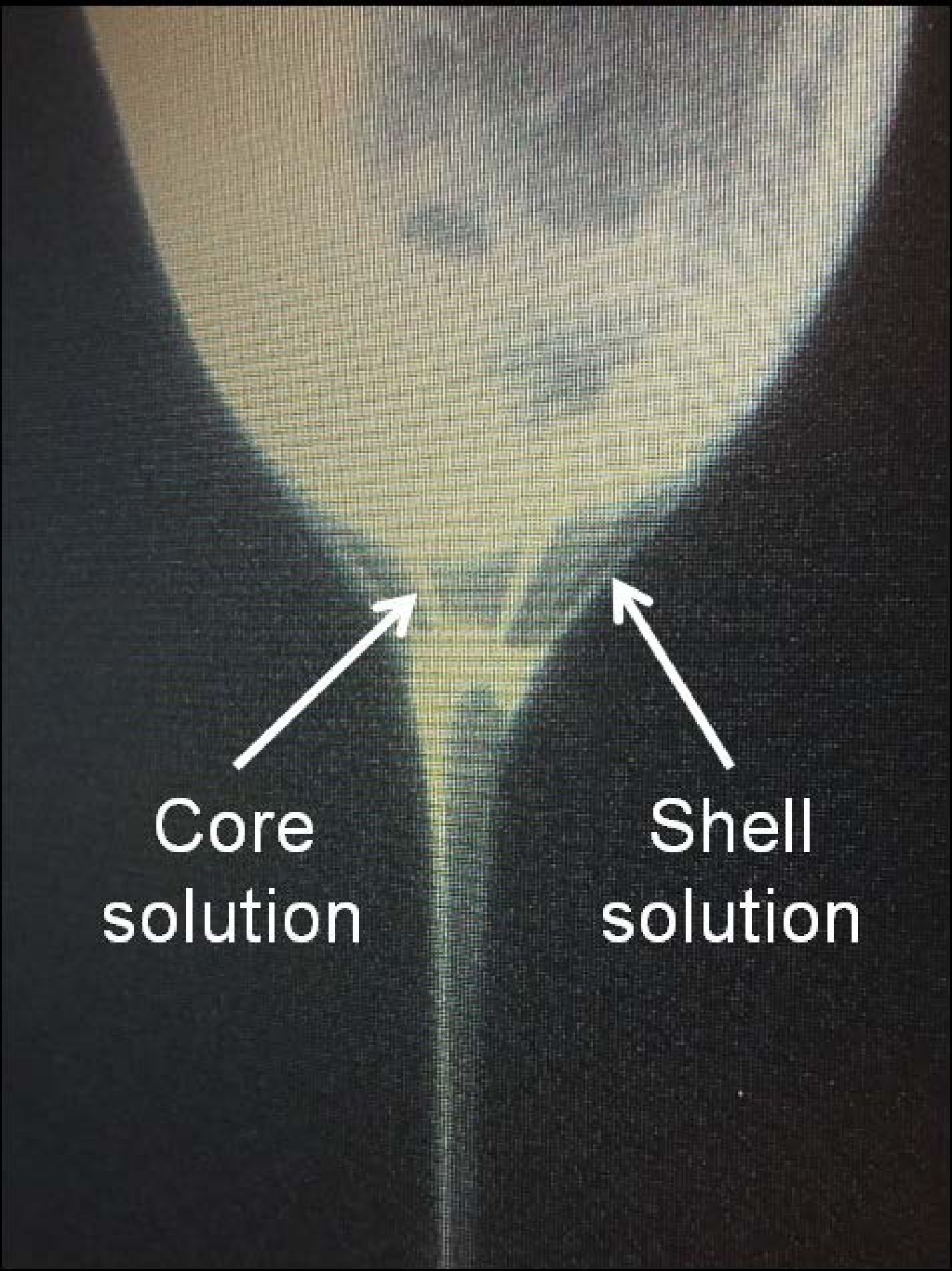
Core
solution
Shell
solution

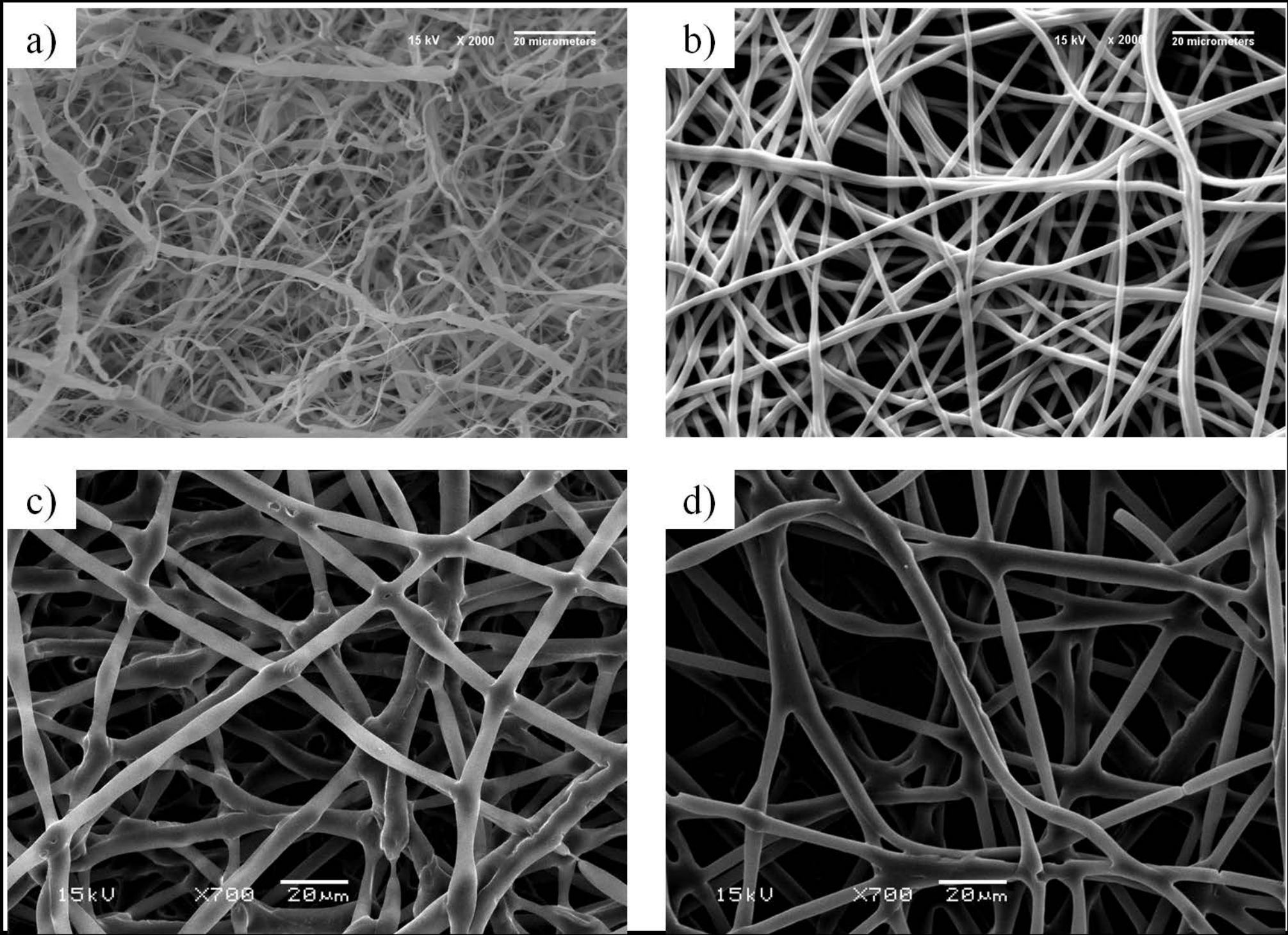
a)
15 kV X 2000 20 micrometers
b)
15 kV x 2000 20 micrometers
c)
15kV X700 20µm
d)
15kV X700 20µm

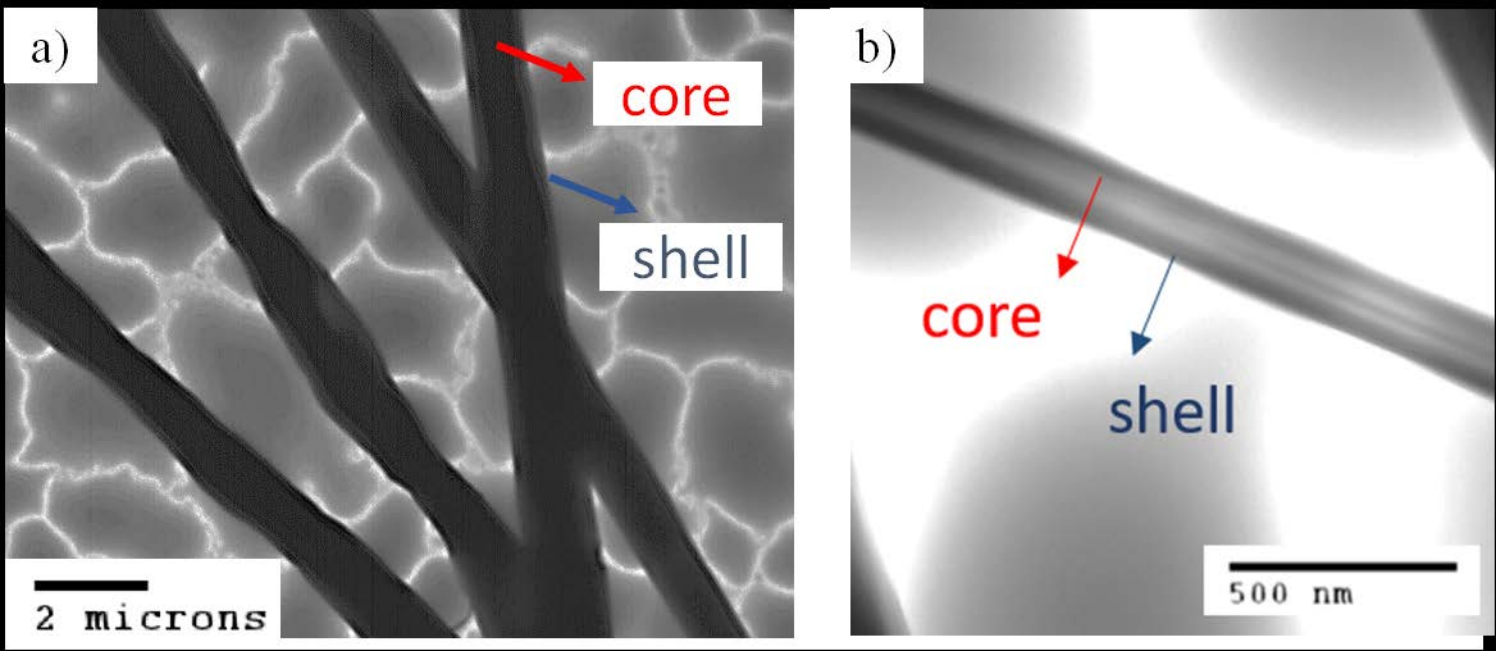
a)
core
shell
2 microns
b)
core
shell
500 nm

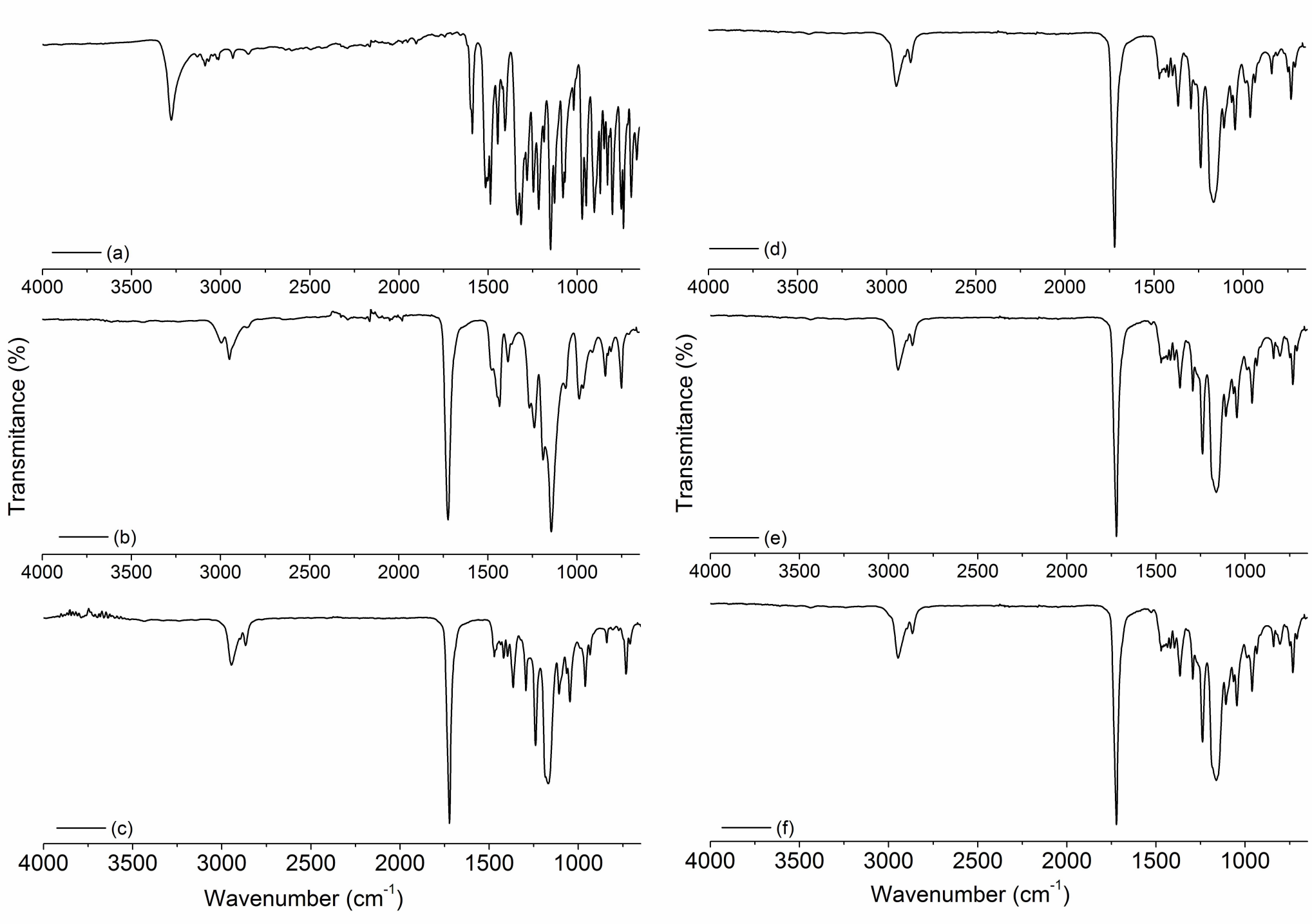
(a)
(b)
(c)
(d)
(e)
(f)
Transmitance (%)
Transmitance (%)
4000
3500
3000
2500
2000
1500
1000
Wavenumber (cm-1)
Wavenumber (cm-1)

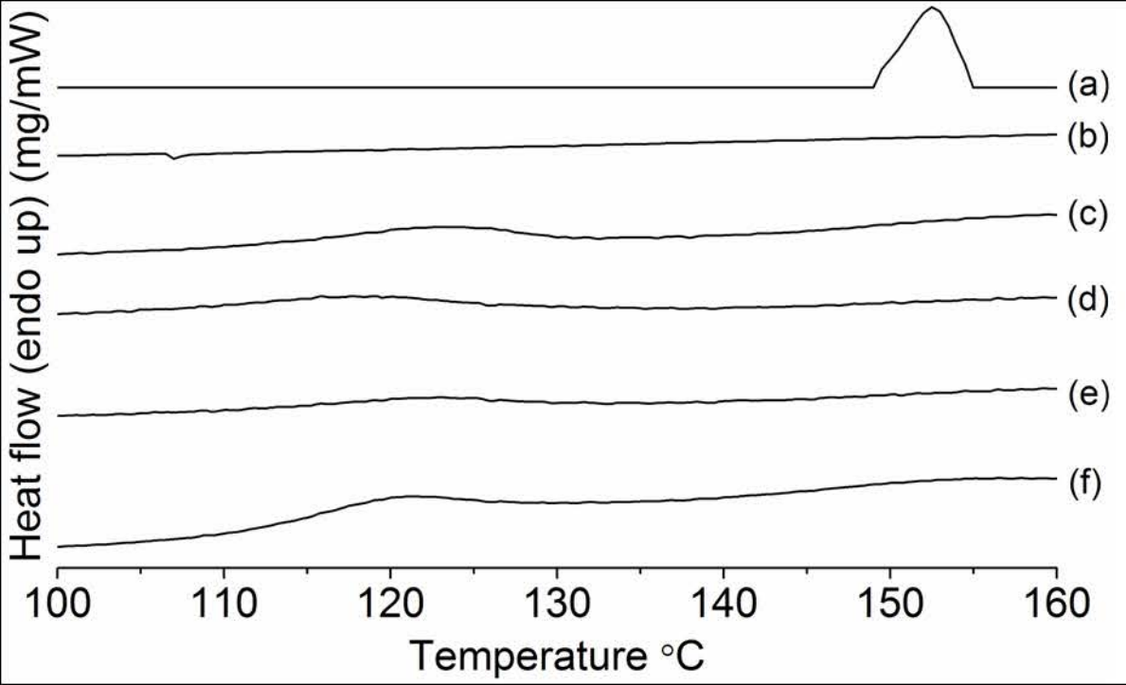
Heat flow (endo up) (mg/mW)
(a)
(b)
(c)
(d)
(e)
(f)
100
110
120
130
140
150
160
Temperature °C

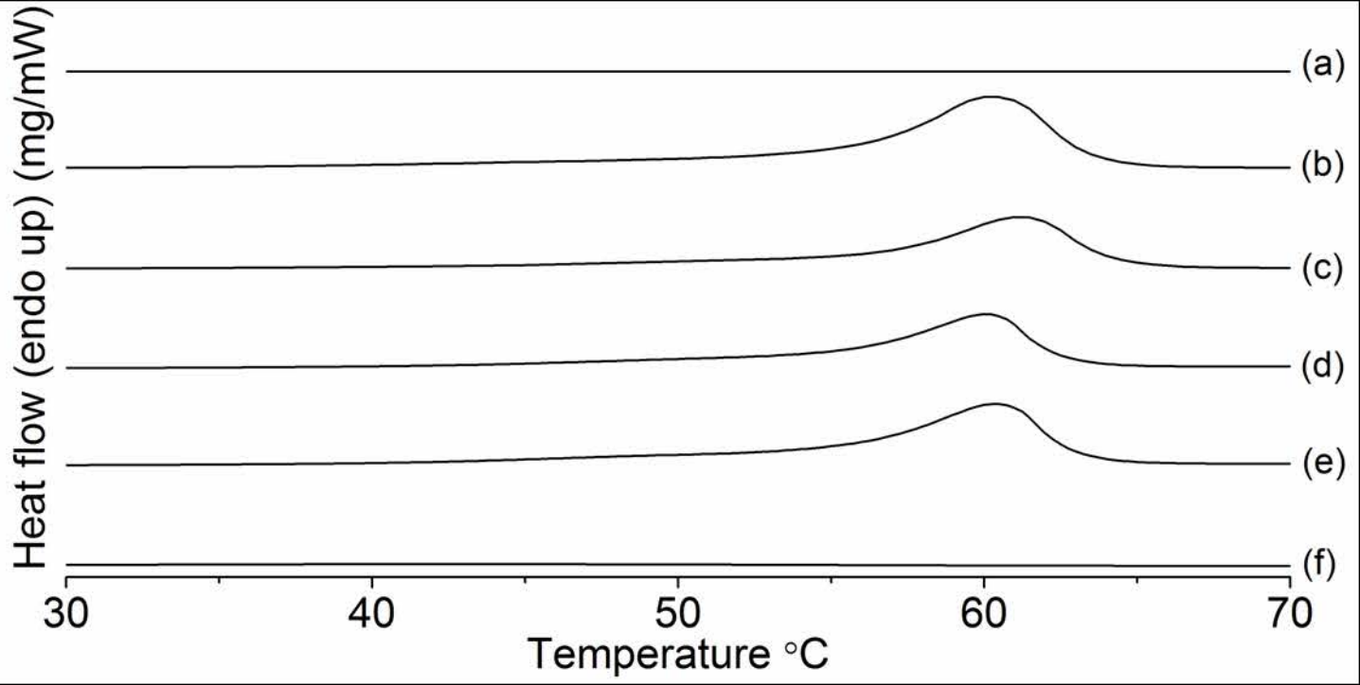
Heat flow (endo up) (mg/mW)
(a)
(b)
(c)
(d)
(e)
(f)
30
40
50
60
70
Temperature °C

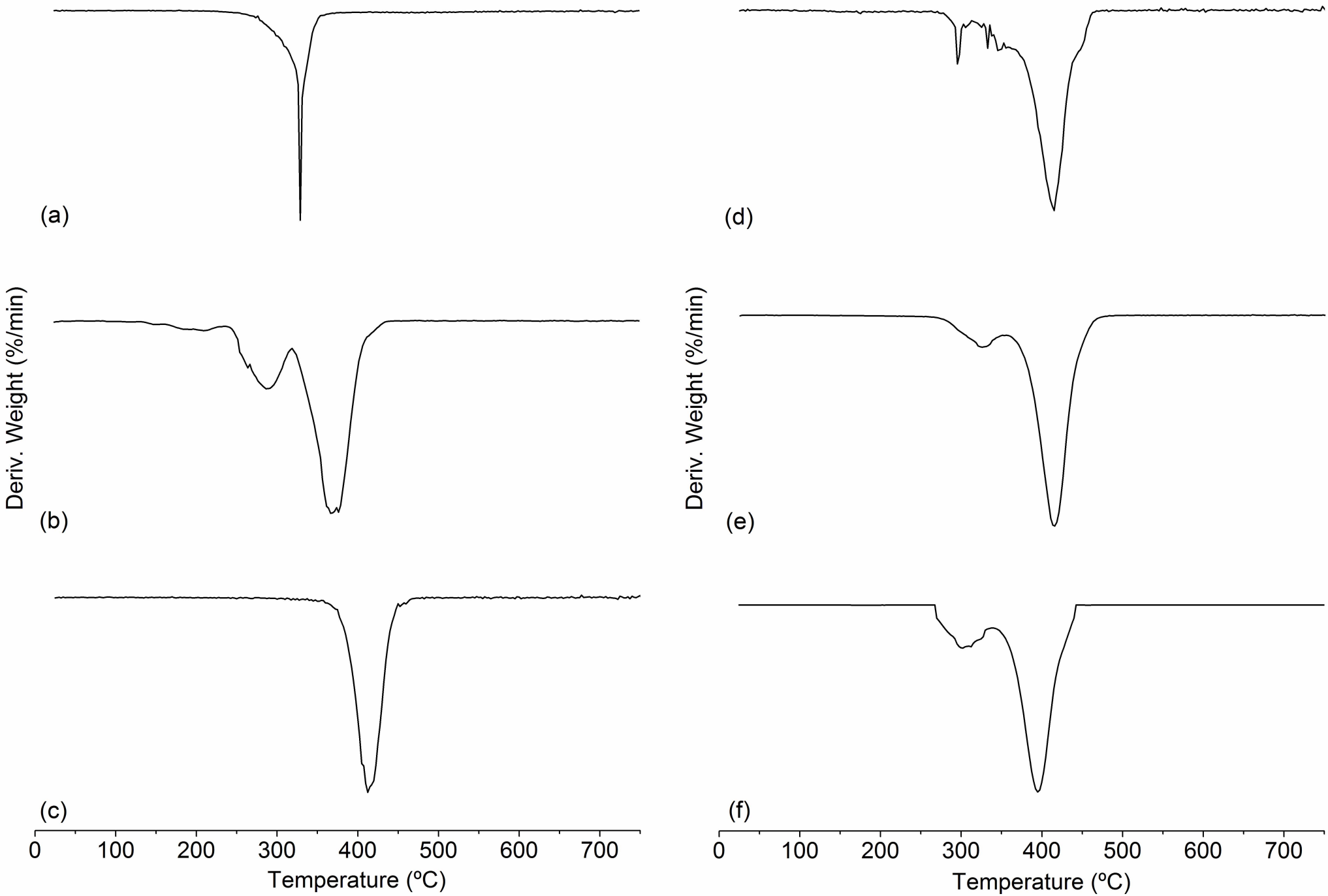
(a)
(b)
(c)
(d)
(e)
(f)
Deriv. Weight (%/min)
Deriv. Weight (%/min)
0
100
200
300
400
500
600
700
Temperature (ºC)
0
100
200
300
400
500
600
700
Temperature (ºC)

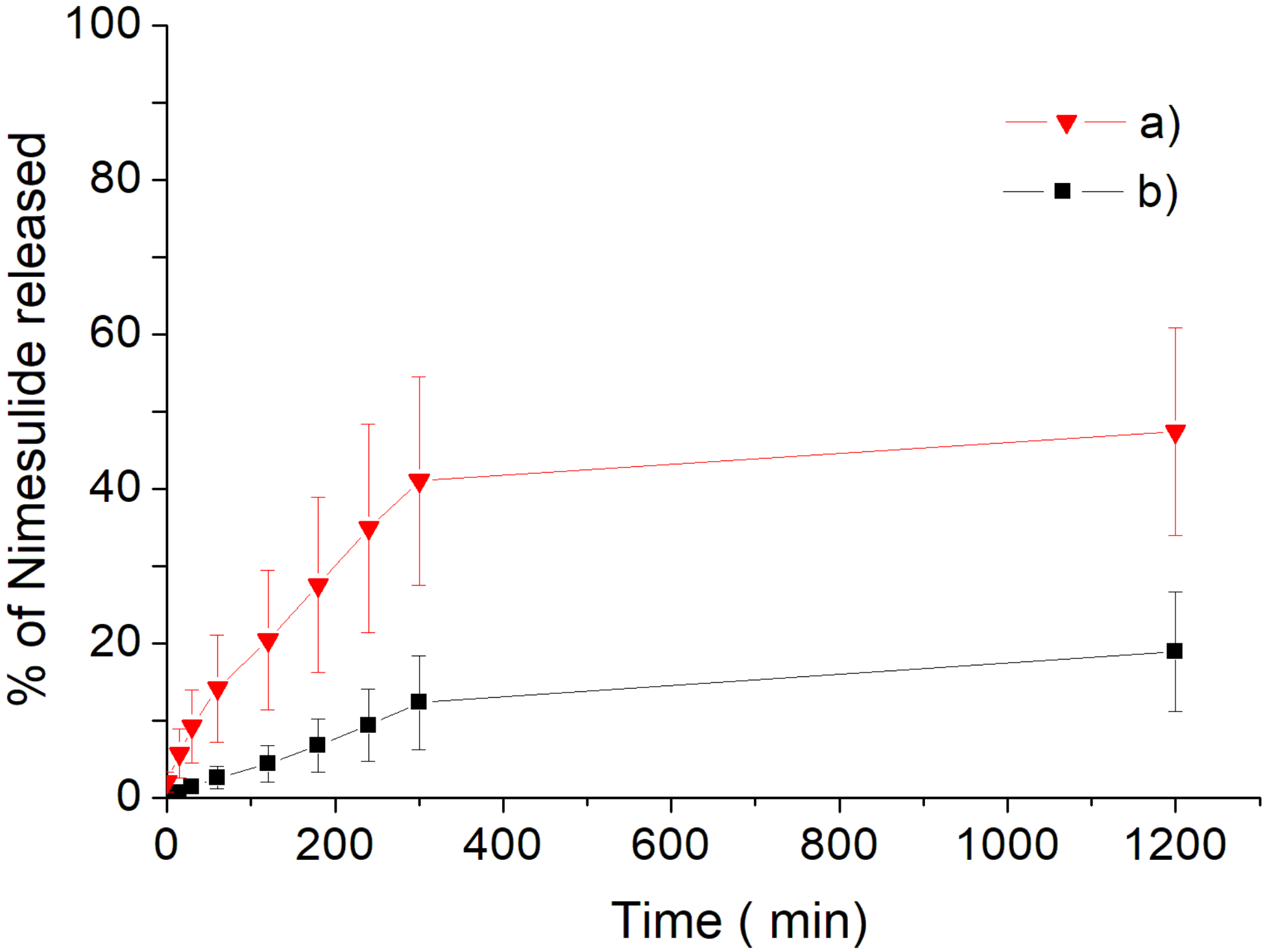
100
80
60
40
20
0
% of Nimesulide released
0
200
400
600
800
1000
1200
Time (min)
a)
b)